GNSS Carrier Tracking Loop : Stability Analysis and Some Improvements

M. Tahir*, U.M. Khurram† and A. Salman‡
Department of Electrical Engineering, Syed Baber Ali School of Science and Engineering,
Lahore University of Management Sciences, Lahore, Pakistan
Email: *tahir@lums.edu.pk, †15100017@lums.edu.pk, ‡15100068@lums.edu.pk

***Abstract*—Carrier tracking loops used in satellite navigation receiver are discrete-time closed loop systems that are mostly designed from their continuous time counterparts. In this paper, we analyze the stability of second order carrier tracking loop, assisted and unassisted versions, when designed from continuous time domain. It is well-known that increasing the product of loop noise bandwidth and integration time, this design approach fails and our resulting discrete time loop becomes unstable. Using Bode analysis technique, we show the effect of variation of loop filter coefficients on stability margin of the loop. Based on the discussion, some improvements have been proposed to increase the stability margin of both unassisted and assisted loops. While considering assisted loop, it is a common misconception that assisted loop is more robust to changes in loop noise bandwidth and integration time product as compared to its unassisted counterpart. We show that this is true only for small values of loop noise bandwidth and integration time product. Monte Carlo simulations verify all the presented results in the paper.**

I. Introduction

In global navigation satellite system (GNSS), relative motion between user and satellite causes time varying Doppler shifts in the received signal. Accurate determination of this Doppler is essential for perfect carrier wipe-off from the incoming signal which is required by delay locked loop (DLL) to make code phase measurements. For this purpose, traditional approach to estimate and then keep track of these time varying Doppler shifts is to deploy phase-locked loops (PLL), frequency locked loops (FLL) or an FLL-assisted-PLL where FLL assists PLL in a strongly coupled manner [1]. Traditional approach to design these tracking loops is to approximate these loops by their continuous time counterparts. The reason to adopt this design method is the simplicity of the method. Another reason is that in continuous time domain, design of these loops has been extensively studied and there exist a lot of design methods for different loop order and types which can conveniently be converted into discrete time domain using continuous time to discrete time transformations like Bilinear transform etc.

These transformations actually approximate the behavior of continuous time loop in discrete time domain. This approximation remains valid only for smaller values of the product of sampling time and loop bandwidth i.e. BT, where B is loop bandwidth and T is the integration time for correlation which is also the update interval of the loop. Actually, the value of this product is directly related to the positions of the closed loop poles in z-plane. When this product starts increasing, the poles start moving towards outside the unit circle. Eventually, the loop becomes unstable for larger BT values and we say that the approximation from continuous time domain to discrete time domain has failed.

On the other hand, GNSS receivers working in harsh environments require larger BT values for tracking loops. This may be the result of either of the following two requirements:

1) Received signal power is very low. In this case, we are interested in increasing the value of T which will enable us to recover even very weak signal.
2) User has very high dynamics. In this case, relative velocity between user and satellite will be very high resulting in larger values of Doppler shift and Doppler rate. In order to track these larger values of Doppler quantities, we need to increase the loop noise bandwidth of the tracking loop.

A lot of work has already been done and is in progress to cope with the design of the loop for larger BT product values. One option is to rely on other techniques of designing digital loops instead of relying on continuous time design choices. For this purpose, some techniques have been proposed in the literature as discussed in [2]. All of these architectures aim either at re-designing or replacing the loop filter with a more robust block. Unfortunately, the design method involved in most of these approaches becomes more intricate and very specific for certain type of user dynamics.

Other alternative is to work around classical approach of designing tracking loops from their continuous time counterparts and try to improve its robustness against larger BT products. So, it becomes essential to completely comprehend the phenomenon which results in loop instability. For this purpose, Bode analysis technique is very useful is analyzing the stability of closed loop system. Recently this technique has been used by GNSS community to address the stability issues of GNSS tracking loops [3], [4]. Performance of the loop and its stability properties strongly depend on the transformation functions used for converting continuous time system to discrete time systems. Two most common transformations used among GNSS community are Bilinear rule and Forward or Boxcar rule. Usual approach is to use Bilinear rule for loop filter and Boxcar rule for numerically controlled oscillator (NCO) which is digital counterpart of voltage controlled oscillator (VCO) [3]. In this paper, we clearly outline the rationale behind this choice and also explore other alternatives. Specifically, we use Bode analysis technique to completely analyze the stability of a second order PLL and its assisted counterpart i.e. second order PLL assisted by first order FLL when designed from continuous

978-1-4799-9969-9/15 $31.00

time loops. We show the following:

- In case of unassisted loop, phase margin can be obtained by considering the open loop transfer function of the closed loop system. For this purpose, a similar approach is adopted as presented in [3].
- In case of assisted loop, open loop transfer function can be obtained by using only one phase discriminator for generation of both phase and frequency errors. In order to generate frequency error, phase discriminator is followed by a differentiator.
- In case of assisted loop, it is better to use Bilinear for differentiator instead of conventional Boxcar model.
- In both assisted and unassisted PLL, the stability margin can be increased significantly by redesigning the loop filter coefficients using Bilinear transform for complete loop and not just for the loop filter by adopting an approach similar to the one presented in [5].
- It is a common misconception that assisted loop is more robust as compared to its unassisted counterpart, we actually show that this is true only for small values of BT product. As this product increases, unassisted loop is more robust in terms of stability margin for a significant range of BT product before loop becomes unstable.
- While considering only assisted loop, PLL is weaker loop as it breaks first thus making whole loop unstable.

All the results obtained from Bode analysis are further verified by developing a Monte Carlo simulation environment.

Rest of the paper is organized as follows. Section II presents some relevant background theory necessary to develop the open loop models which will be used to obtain phase margin for stability analysis. Section III presents analysis and simulation results that support the developed models in previous sections. Based on the discussion in this section, some conclusions are drawn in section IV.

II. Second Order Tracking Loop Theory

A. s-domain:

General block diagram of a GNSS tracking loop in Laplace domain is shown in Fig. 1. NCO $N(s)$ is responsible for generating a local replica of the incoming phase. Assuming unity gain, NCO is modeled as an integrator in s-domain such that

$$N(s) = \frac{1}{s} \tag{1}$$

The locally generated phase is then compared with incoming phase by loop discriminator $LD(s)$ to detect the phase error between them. Zero-order model for loop discriminator is simply a gain k_d which can be assumed unity without loss of generality such that

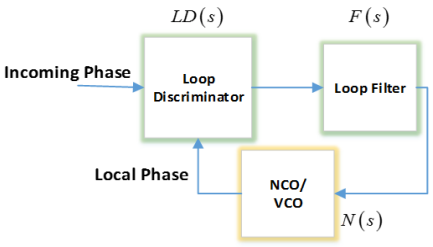

Fig. 1: GNSS tracking loop in s-domain

$$LD(s) = k_d = 1 \tag{2}$$

Order and type of the closed loop system is determined by the choice of loop filter $F(s)$ which is more a controller than simply a filter. Its role as controller has already been outlined in literature [2]. We consider following choices for $F(s)$ in this paper:

- **First order loop:** For first order loop, $F(s)$ is simply a proportional constant i.e.

$$F_1(s) = f_1 \tag{3}$$

  where $f_1 = \omega_o =$ Natural frequency of the loop which is also related to loop noise bandwidth B of first order loop as $B = 0.25\omega_o$
- **Second order loop:** For second order loop, $F(s)$ is proportional-integrator (PI) controller i.e.

$$F_2(s) = c_1 + \frac{c_2}{s} \tag{4}$$

  where c_1 and c_2 are related to 2nd order loop parameters ω_o and ζ as $c_1 = 2\zeta\omega_o$ and $c_2 = \omega_o^2$. Here, ω_o is again natural frequency of the loop which is related to loop noise bandwidth B of second order loop as $B = 0.53\omega_o$ and ζ is the damping ratio.
- **2nd order assisted loop:** Most common structure of 2nd order assisted loop used in GNSS is 2nd order PLL assisted with 1st order FLL which can be modeled as shown in Fig. 3. Notice that, FLL architecture is different from PLL as in this case phase discriminator is preceded by a differentiator, $D(s)$ which generates frequency error from phase error, which is then followed by an integrator, $\frac{1}{s}$ in the remaining loop. Also the use of single discriminator for both phase and frequency error detection may cause phase outlier to affect the frequency estimation but this can be avoided by redesigning phase discriminator as given in [6]. In our approach, we will consider an alternate structure for assisted loop as shown in Fig. 3 which is mathematically equivalent to Fig. 2. Using this model, we can include $D(s)$ and integrator in FLL chain in the loop filter such that

$$F_a(s) = D(s)\frac{f_1}{s} + \left(c_1 + \frac{c_2}{s}\right) \tag{5}$$

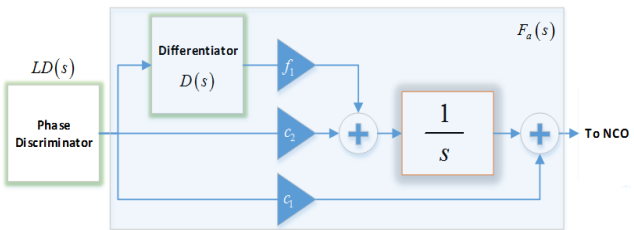

Fig. 2: Loop filter for assisted loop

Assuming proper values for different gains, we can write closed loop transfer function for first and second order loops

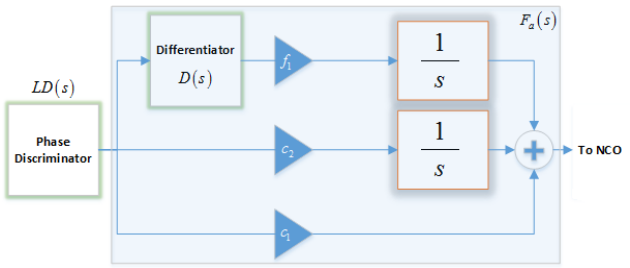

Fig. 3: Equivalent structure for assisted loop filter

as:

$$H_1(s) = \frac{F_1(s)N(s)}{1 + F_1(s)N(s)} = \frac{f_1}{s + f_1} \tag{6}$$

$$H_2(s) = \frac{c_1 s + c_2}{s^2 + c_1 s + c_2} \tag{7}$$

Equations (6) and (7) will be used to find values of f_1, c_1 and c_2 for all three filters.

B. Moving from s-Domain to z-domain:

Following two transformations are mostly used to convert continuous time transfer function to an equivalent discrete time transfer function:

- **Bilinear:**

$$s \rightarrow \frac{2}{T}\frac{1 - z^{-1}}{1 + z^{-1}} \tag{8}$$

- **Boxcar:**

$$s \rightarrow \frac{1 - z^{-1}}{Tz^{-1}} \tag{9}$$

where T corresponds to sampling interval i.e. update interval in the loop. It is widely known that Bilinear rule is much better as compared to other transformations. So, one might aim to use Bilinear for each individual block while transforming a continuous time loop to discrete time loop. However, as discussed below, we can not use Bilinear for all the blocks inside closed loop system.

z-domain model of a discrete time tracking loop used in GNSS receivers is shown in Fig. 4. Here, we have an additional block as compared to its analog counterpart, integrate and dump $ID(z)$ which accumulates number of samples over each integration period T and outputs a complex quantity. Phase of this quantity is the average phase difference between incoming and local carriers over integration interval T. We can model these blocks in z-domain as discussed below. NCO is traditionally modeled

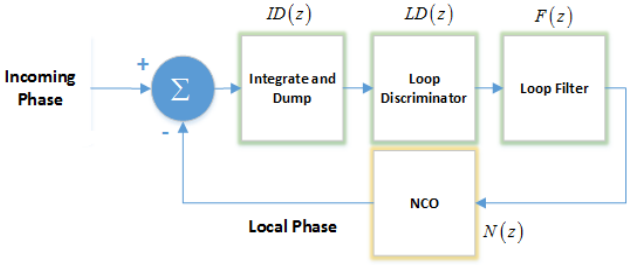

Fig. 4: GNSS tracking loop in z-domain

using Boxcar rule which results in

$$N(z) = \frac{Tz^{-1}}{1 - z^{-1}} = \frac{T}{z - 1} \tag{10}$$

Notice that, we need to incorporate an inherent delay in any of the block inside the loop due to its discrete time nature. It can be shown easily that only Boxcar rule allows us to have such a delay element in the obtained discrete time loop transfer function. NCO is usually chosen for this purpose. However, we will show that we can *emulate* Bilinear rule for NCO by properly modifying filter coefficients to include this effect. This is an indirect modeling of NCO by Bilinear transform which results in sufficient advantage in terms of stability margin.

Integrate and dump block is modeled directly in z-domain as [3]

$$ID(z) = \frac{1 + z^{-1}}{2} \tag{11}$$

Loop discriminator $LD(z)$ is again modeled as a constant in z-domain. Loop filter $F(z)$ is always modeled using Bilinear transform which results in

$$F_1(z) = f_1 \tag{12}$$

$$F_2(z) = \frac{a_1 + a_2 z^{-1}}{1 - z^{-1}} \tag{13}$$

with $a_1 = c_1 + 0.5Tc_2$ and $a_2 = 0.5Tc_2 - c_1$. In case of assisted loop, $F_a(z)$ depends on how we model differentiator i.e. $D(s)$ in z-domain. For a general expression for $D(z)$, we get

$$F_a(z) = f_1 D(z)\left(\frac{T}{2}\frac{1 + z^{-1}}{1 - z^{-1}}\right) + \frac{a_1 + a_2 z^{-1}}{1 - z^{-1}} \tag{14}$$

Now, if we replace $D(s)$ in z-domain by Bilinear, we get

$$F_a(z) = f_1 + \frac{a_1 + a_2 z^{-1}}{1 - z^{-1}} \tag{15}$$

and if we chose Boxcar model for $D(s)$, which is the usual approach to find frequency error from phase error, we get

$$F_a(z) = f_1\left(\frac{1}{2}\frac{1 + z^{-1}}{z^{-1}}\right) + \frac{a_1 + a_2 z^{-1}}{1 - z^{-1}} \tag{16}$$

C. Bilinear model for NCO:

As already stated, direct mapping of NCO using Bilinear transform is not possible because in that case, in order to compute current replica of the phase at NCO output, we will be needing that frequency value from loop filter which is still to be computed using current NCO phase in the next update interval. This is an inherent problem of any digital feedback loop. But still we can indirectly model it by modifying the loop filter coefficients to include this effect.

1) Calculating f_1: Starting from closed loop transfer function of first order loop given in (6), we can use Bilinear on $H_1(s)$ to get corresponding closed loop transfer function in z-domain $H_1(z)$ as shown below.

$$H_1(z) = H_1(s)\big|_{s=\frac{2}{T}\frac{1-z^{-1}}{1+z^{-1}}} \tag{17}$$

$$= \left(\frac{\omega_o}{s + \omega_o}\right)\Big|_{s=\frac{2}{T}\frac{1-z^{-1}}{1+z^{-1}}} \tag{18}$$

$$= \frac{2\omega_o(z - 1)}{(2 + T\omega_o)z - (2 - T\omega_o)} \tag{19}$$

We can also form closed loop transfer function of first order loop directly in z-domain referring to Fig. 4 and using (10) and (12),

$$H_{1_z}(z) = \frac{F_1(z)N(z)}{1 + F_1(z)N(z)} \tag{20}$$

where $LD(z)$ has been assumed unity and $ID(z)$ has not been considered as this block is not present in analog counterpart. Now, substituting the expressions, we get

$$H_{1_z}(z) = \frac{f_1 \frac{T}{z-1}}{1 + f_1 \frac{T}{z-1}} \tag{21}$$

Notice that here, we will treat f_1 as unknown whose value will be determined by matching the poles of (21) with those of (19). Comparing (21) with (19), we get

$$f_1 = \frac{2\omega_o}{2 + T\omega_o} \tag{22}$$

This is the modified value of first order loop filter coefficient. This value, when used with Boxcar NCO, will give us overall loop which will behave as every block has been transformed to z-domain using Bilinear.

Note that, when T is very small, we have $2 >> (T\omega_o)$. We can say that $2 + T\omega_o \approx 2$ such that the value of f_1 in (22) reduces to its traditional value i.e. ω_o.

2) Calculating c_1 and c_2: A similar procedure can be adopted for 2nd order loop to calculate its modified coefficients. The results are outlined below,

$$H_2(z) = H_2(s)\Big|_{s=\frac{2}{T}\frac{1-z^{-1}}{1+z^{-1}}} \tag{23}$$

$$= \left(\frac{2\zeta\omega_o s + \omega_o^2}{s^2 + 2\zeta\omega_o s + \omega_o^2}\right)\Bigg|_{s=\frac{2}{T}\frac{1-z^{-1}}{1+z^{-1}}} \tag{24}$$

which can be simplified to

$$H_2(z) = \frac{[4\zeta\omega_o T + (\omega_o T)^2] + 2(\omega_o T)^2 z^{-1} + [(\omega_o T)^2 - 4\zeta\omega_o T] z^{-2}}{[4 + 4\zeta\omega_o T + (\omega_o T)^2] + [2(\omega_o T)^2 - 8] z^{-1} + [4 - 4\zeta\omega_o T + (\omega_o T)^2] z^{-2}} \tag{25}$$

Similarly, using (13) and (10), we can obtain $H_{2_z}(z)$ as

$$H_{2_z}(z) = \frac{F_2(z)N(z)}{1 + F_2(z)N(z)} \tag{26}$$

$$H_{2_z}(z) = \frac{T(c_1 + 0.5c_2T)z^{-1} + T(0.5c_2T - c_1)z^{-2}}{1 + [T(c_1 + 0.5c_2T) - 2]z^{-1} + [1 + T(0.5c_2T - c_1)]z^{-2}} \tag{27}$$

Here, we again treat c_1 and c_2 as unknowns. Now, comparing (25) and (27), we get,

$$c_1 = \frac{8\zeta\omega_o + 2\omega_o^2 T}{4 + 4\zeta\omega_o T + (\omega_o T)^2} \tag{28}$$

$$c_2 = \frac{4\omega_o^2}{4 + 4\zeta\omega_o T + (\omega_o T)^2} \tag{29}$$

Again, it is interesting to note that both c_1 and c_2 reduce to their traditional values of $2\zeta\omega_o$ and ω_o^2 respectively, when T is very small.

D. Open loop transfer function:

Fig. 5 presents open loop model of GNSS carrier tracking loop adopted for the purpose of phase margin analysis using Bode analysis technique. The loop has been opened after integrate and dump block as shown in Fig. 5, by assuming all signals external to the loop equal to zero as required by this technique. Now, we can find open loop transfer function $G(z)$ for the loop and corresponding phase margin for stability analysis.

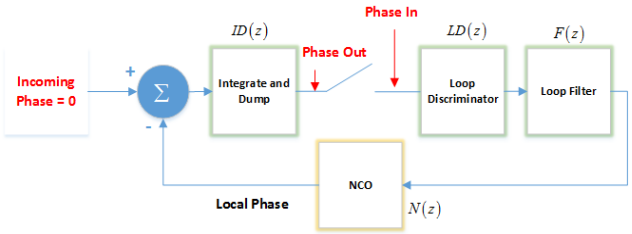

Fig. 5: GNSS tracking loop under Bode test condition

$$G(z) = LD(z)F(z)N(z)ID(z) = \frac{T}{2}z^{-1}\left(\frac{1 + z^{-1}}{1 - z^{-1}}\right)F(z) \tag{30}$$

where $F(z)$ can take any of the following forms, depending on order and type of the loop,

- **First order loop:** $F(z) = F_1(z)$ given in (12) with possible choices for f_1 outlined in Table I.

TABLE I: Coefficients for $F_1(z)$

	f_1
Traditional	ω_o
Modified	$\frac{2\omega_o}{2+T\omega_o}$

- **Second order loop:** $F(z) = F_2(z)$ given in (13) with possible choices for c_1 and c_2 outlined in Table II.

TABLE II: Coefficients for $F_2(z)$

	c_1	c_2
Traditional	$2\zeta\omega_o$	ω_o^2
Modified	$\frac{8\zeta\omega_o + 2\omega_o^2 T}{4+4\zeta\omega_o T+(\omega_o T)^2}$	$\frac{4\omega_o^2}{4+4\zeta\omega_o T+(\omega_o T)^2}$

- **Second order assisted loop:** $F(z) = F_a(z)$ given in (15) or (16) depending on the model for $D(z)$ with possible choices for f_1, c_1 and c_2 outlined in Table III.

TABLE III: Coefficients for $F_a(z)$

	f_1	c_1	c_2
Traditional	ω_o	$2\zeta\omega_o$	ω_o^2
Modified	$\frac{2\omega_o}{2+T\omega_o}$	$\frac{8\zeta\omega_o + 2\omega_o^2 T}{4+4\zeta\omega_o T+(\omega_o T)^2}$	$\frac{4\omega_o^2}{4+4\zeta\omega_o T+(\omega_o T)^2}$

At this point, we can analyze the stability of the loop in terms of phase margin using (30) considering different choices for $F(z)$.

III. Results and Discussion

In this section, we present the results obtained analyzing the models discussed in section II. We consider only 2nd order PLL - unassisted and assisted by first order FLL. A mechanism has also been developed to verify the presented results using Monte Carlo simulations. In all the presented results, unstable region corresponds to the region where phase margin becomes negative. Before unstable region, the response of the loop is highly distorted in some proximate region rendering the loop unfit for practical use. This region has been termed as distorted region in the results.

978-1-4799-9969-9/15 $31.00 ©2015 IEEE

A. Traditional vs. modified coefficients:

Considering unassisted 2nd order PLL, phase margin is obtained using (30) with $F(z)$ given in (13). Two cases are considered: traditional and modified coefficient as outlined in Table II. The results are shown in Fig. 6 for a fixed value of loop noise bandwidth B while varying integration time T. It is clear that modified coefficients provide us significant improvement in terms of stability margin as compared to traditional coefficient case. This is intuitive as we have already discussed that modified coefficients model digital loop more accurately specially when we are working with larger update intervals T. For smaller values of T, performance in both cases is almost same.

For assisted loop, we can obtain phase margin using (30) with $F(z)$ given in (16) which models differentiator in digital domain using Bilinear approximation. Again, we consider both cases. The results are again presented in Fig. 6. Again, we observe significant improvement in terms of stability margin.

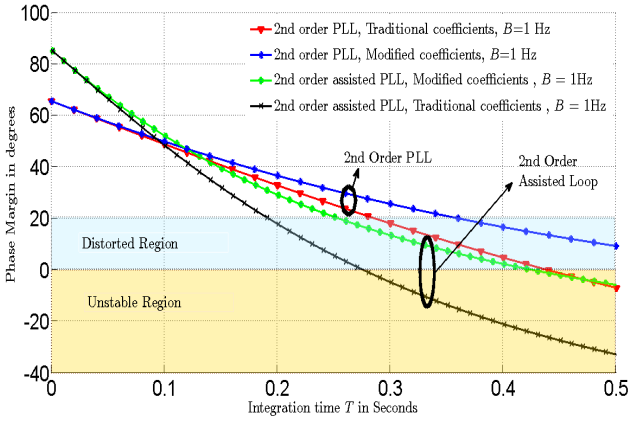

Fig. 6: Phase margin of 2nd order loops

B. Assisted vs. unassisted loop:

Fig. 6 provides comparison between assisted and unassisted loops under same parameter settings. It is clear that assisted loop is more robust as compared to its unassisted counterpart for smaller BT products. As T increases, stability margin of assisted loop decreases faster as compared to unassisted loop, thus making it more vulnerable. This aspect clearly indicates that assisted loop is not always robust as compared to unassisted loop, rather only for smaller BT product values.

C. Assisted loop: Boxcar vs. Bilinear differentiator

In case of assisted loop, another useful comparison can be made between (15) and (16) where in former case, Bilinear is used to replace $D(s)$ in z-domain and in later case Boxcar is used. The results are shown in Fig. 7. These results have been obtained by considering traditional coefficients for both PLL and FLL in assisted loop. Loop noise bandwidths of both PLL and FLL is set to 1 Hz while integration time is varied. Similar results can also be obtained using modified coefficients. It is clear that choice of Bilinear for differentiator offers significant stability margin improvement as compared to Boxcar case.

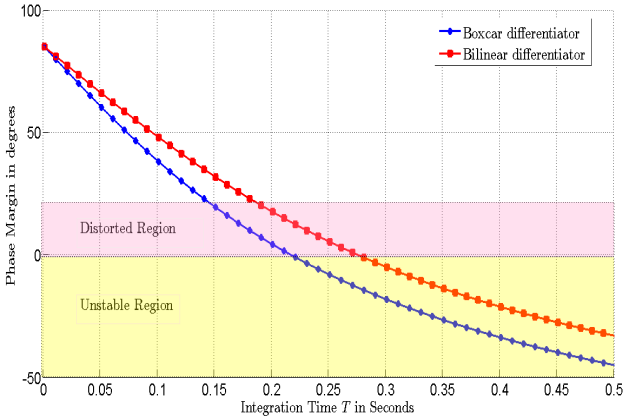

Fig. 7: Phase margin of assisted loop with different models for $D(s)$ and traditional coefficients for loop filter

D. Assisted loop: PLL vs. FLL

In case of assisted loop, we can identify the more vulnerable loop between PLL and FLL to changes in BT product. For this purpose, we keep integration time constant and vary loop noise bandwidth of both PLL and FLL alternatively. The results are presented in Fig. 8 for traditional loop coefficients and Bilinear model for differentiator in all cases. In any of these curves, BT product for one loop is constant and for other loop is varying. Under this setting, if assisted loop breaks it is clear that it is only due to that loop for which BT product was varying. From results, it is observed that PLL is weaker loop as it breaks first making whole loop unstable while FLL is more robust.

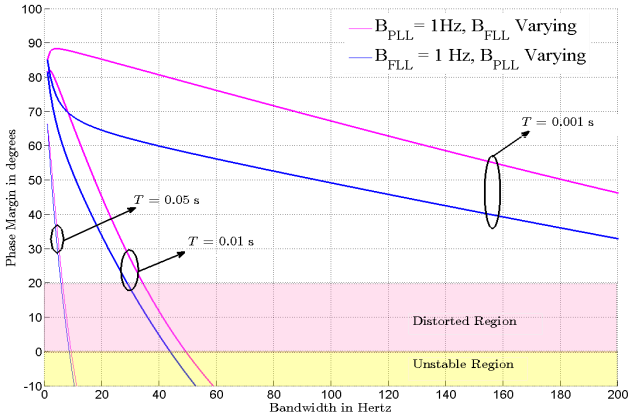

Fig. 8: Phase margin of assisted loop by varying loop noise bandwidth of FLL or PLL

E. Verifying the results: Monte Carlo simulations

In order to verify the presented results, we can develop a Monte Carlo simulation to measure some parameter in time domain response of the loop that is directly related to phase margin and hence in a sense can be used to quantify loop stability margin. For this purpose, we have considered to measure the percentage overshoot of the step response of the closed loop system which is related to damping ratio of the loop which in turn is related to phase margin [7]. Following procedure has been developed to measure the percentage overshoot using simulations:

978-1-4799-9969-9/15 $31.00 ©2015 IEEE

- *Step 1:* GNSS like signal of certain duration is generated considering a sufficient higher value for carrier to noise ratio, C/N_o assuming code has been perfectly wiped-off. The value of Doppler is chosen to be a step.
- *Step 2:* This signal is fed to the carrier tracking loop which is under consideration for some parameter settings. Doppler estimates at the output of the loop filter are considered for percentage overshoot measurement.
- *Step 3:* Percentage overshoot is measured and this process is repeated for a number of iterations. At each value of iteration, Doppler step is kept same but signal is generated a new.
- *Step 4:* At the end of all iterations, an average value of percentage overshoot is recorded and stored for current settings of the loop.
- *Step 5:* This process is repeated for each value of the loop parameter and results are plotted at the end.

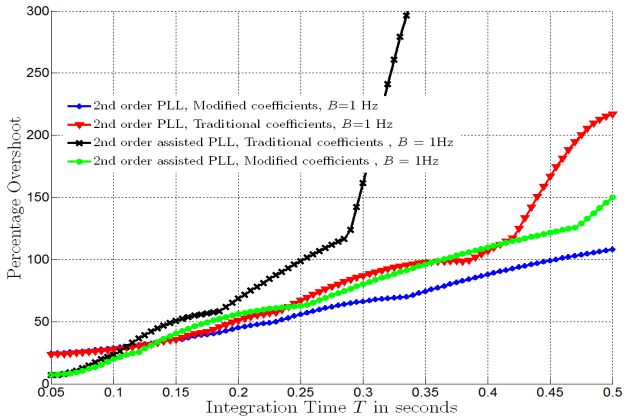

Fig. 9: Percentage overshoot corresponding to different loops

Fig. 9 presents simulation results plotting percentage overshoot for all the cases presented in Fig. 6. These results are presented starting from sufficiently higher value of integration time T because the presence of noise makes it difficult to measure the percentage overshoot for relatively smaller T values. Larger percentage overshoot indicates the loop has less stability margin and hence it is more close to becoming unstable. The trends in Fig. 9 are very much in agreement with those in Fig. 6, and hence verify all the analysis results. Similarly, all other analysis results have also been verified following the same procedure as described for this case.

IV. Conclusion

Stability of 2nd order carrier tracking loop has been analyzed using Bode analysis technique. It has been shown that the choice of different continuous-time to discrete-time approximations directly impacts the stability of the loop. We have shown that redesigning loop filter coefficients by considering Bilinear model for all the blocks in continuous time loop results in significant stability margin improvement. Assisted loop is more robust only for smaller values of BT products as compared to unassisted loop. Some improvements have been suggested in assisted loop by carefully choosing the model for differentiator in FLL chain. Presented results have been verified using Monte Carlo simulations.

References

[1] E. Kaplan and C. Hegarty, Eds., *Understanding GPS Principles and Applications*. Norwood, MA: Artech House, 2006.

[2] M. Tahir, L. Lo Presti, and M. Fantino, "A novel quasi-open loop architecture for GNSS carrier recovery systems," *International Journal of Navigation and Observation*, pp. 1–12, 2012.

[3] P. Ward and T. Fuchser, "Stability Criteria for GNSS Receiver Tracking Loops," in *Proceedings of the 26th International Technical Meeting of The Satellite Division of the Institute of Navigation (ION GNSS+ 2013)*, Nashville, TN, September 2013, pp. 2786–2806.

[4] T. Jin and J. Ren, "Stability analysis of gps carrier tracking loops by phase margin approach," *GPS Solutions*, vol. 17, no. 3, pp. 423–431, 2013. [Online]. Available: http://dx.doi.org/10.1007/s10291-012-0290-8

[5] Y. Jiang, S. fang Zhang, K. Zheng, and Q. Hu, "Analysis and optimum design of loop filter in gnss receiver," in *Intelligent Control and Automation (WCICA), 2012 10th World Congress on*, July 2012, pp. 2491–2496.

[6] Pedro A. Roncagliolo, Javier G. Garca, and Carlos H. Muravchik, "Optimized Carrier Tracking Loop Design for Real-Time High-Dynamics GNSS Receivers," *International Journal of Navigation and Observation*, vol. 2012, no. 651039, p. 18, 2012.

[7] Norman S. Nise, *Control Systems Engineering*, 6th ed. John Wiley & Sons, Inc., 2011.

978-1-4799-9969-9/15 $31.00